STAR experiment results from BES program

A. Korobitsin[1] *for the STAR collaboration*

Joint Institute for Nuclear Research, 6 Joliot-Curie St., Dubna, Moscow Region, Russia, 141980

One of the primary goals of STAR's experimental program at the Relativistic Heavy-Ion Collider (RHIC) is the investigation of Quantum chromodynamics (QCD) phase properties. These include the search for the location of QCD critical point and the predicted first order phase transition between Quark Gluon Plasma (QGP) and hadron gas. To make a detailed scan on the phase diagram, RHIC has performed two phases of the Beam Energy Scan program colliding gold nuclei at various nucleon-nucleon center of mass energies over the range from 62.4 GeV to 7.7 GeV in BES-I, from 54.4 GeV to 7.7 GeV in BES-II in collider mode and from 13.7 GeV to 3 GeV in fixed-target (FXT) mode.

This report will summarize some of the results obtained from BES-I and BES-II.

PACS: 13.85.–t; 14.20.–c; 25.75.–q

Introduction

The STAR experiment launched a Beam Energy Scan (BES) program for detailed investigation of the QCD phase structure during 2010. The first phase of this program provided experimental data in Au+Au collisions at nucleon-nucleon center of mass energy ($\sqrt{s_{NN}}$) range $7.7-62.4$ GeV, but was limited by both detector and accelerator capabilities providing limited statistics especially at the lowest collision energy. In order to make high statistics measurements of the observables at low collision energies it was necessary to increase the luminosities of RHIC at these energies. STAR's scientific program is enabled by the combination of increased luminosities and detector upgrades for Beam Energy Scan phase II (BES-II) and Fixed-Target (FXT) program. The BES-II upgrades include three detector upgrades: replacement of the inner sectors of STAR Time Projection Chamber (TPC), installation of the end-cap Time-of-Flight (TOF) system and the Event Plane Detector (EPD). Those upgrades significantly increased the detector acceptance and tracking capabilities. In the collider mode, the lowest energy for Au+Au collisions that RHIC can run with adequate luminosity is 7.7 GeV, whereas in the fixed-target mode this low energy limit can be extended to $\sqrt{s_{NN}} = 3$ GeV.

Data taking for the BES-II/FXT program was completed in 2021. Figure 1 shows a bar chart of the BES-II/FXT data sets recorded and compares the new datasets to the older BES-I data. Also shown in the figure are the energies for which we have overlapping coverage from both the collider and

[1]E-mail: koroaa@jinr.ru

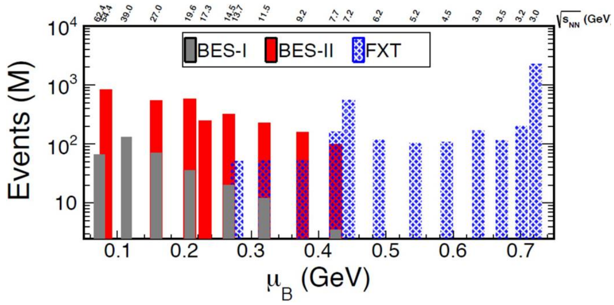

Fig. 1. A summary of the good events acquired for the various collision energies (translated to the baryon chemical potential $\mu_{\rm B}$). The BES-II collider data sets are shown in red bars. The FXT data sets are shown in hashed blue bars. For comparison the BES-I data sets are shown in grey bars. Note that the top FXT energy ($\sqrt{s_{NN}}$ = 13.7 GeV) does not quite overlap with the 14.6 GeV collider system; that FXT energy is a single beam energy of 100 GeV, which is the top energy to which RHIC can accelerate Au ions.

FXT programs. All BES-II collider energies have $10-20$ times higher statistics compared to BES-I. All FXT energies have at least 100 million events (500 million at 7.2 GeV, 2 billion at 3 GeV).

In this proceedings, we report the beam energy dependence of various observables based on BES-I and part of BES-II/FXT data: hyper-nuclei production, femtoscopic measurements, global hyperon polarization measurements and nuclear modification factor.

Hypernuclei production

STAR has performed a series of measurements of the hypernuclei properties, such as lifetime and mass. Hypernuclei are loosely bound and are believed to be produced via the coalescence mechanism during the final stages of the fireball when it has cooled enough to allow hypernuclei to escape the medium without dissociating to their constituents. Precise measurements of ${}^{3}_{\Lambda}H$ and ${}^{4}_{\Lambda}H$ lifetimes have been obtained using the data samples of Au+Au collisions at energies $\sqrt{s_{NN}} = 3$ and 7.2 GeV. The lifetimes are measured to be $221 \pm 15(stat.) \pm 19(syst.)$ ps for ${}^{3}_{\Lambda}H$ and $218 \pm 6(stat.) \pm 13(syst.)$ ps for ${}^{4}_{\Lambda}H$. Figure 2 shows the comparison of world data on measured lifetimes for ${}^{3}_{\Lambda}H$ and ${}^{4}_{\Lambda}H$ from previous measurements and theoretical calculations [1]. Results for both hypernuclei are noticeably different from the lifetime of free Λ baryon.

The p_T-integrated yields of ${}^{3}_{\Lambda}H$ at mid-rapidity were calculated for central collisions as a function of center-of-mass energy. Figure 3 shows dependence of ${}^{3}_{\Lambda}H$ yields within $|\eta| < 0.5$ on the beam energy in $0-10\%$ central heavy-ion collisions. The full red and black square symbols represent STAR preliminary results. Figure 3 demonstrated a significant enhancement compared to the results at 2.76 TeV from ALICE experiment [2], which can be explained by the increase in baryon density at low energies. The result was compared to

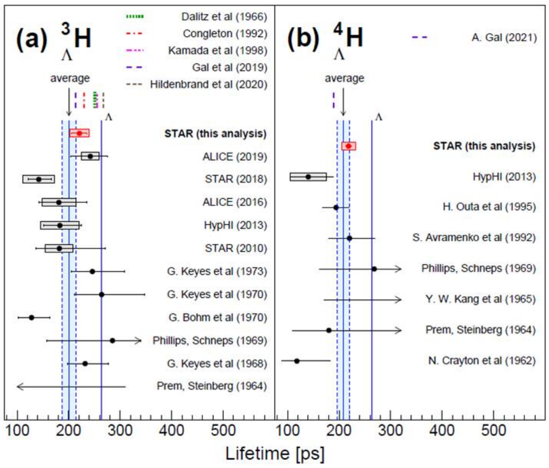

Fig. 2. Measured lifetimes of $^{3}_{\Lambda}H$ and $^{4}_{\Lambda}H$ from different experiments. Horizontal lines represent statistical uncertainties, while boxes represent systematic uncertainties. Vertical blue bands represent the average lifetimes of $^{3}_{\Lambda}H$ and $^{4}_{\Lambda}H$ and free Λ baryon. Data are taken from the paper [1].

several model predictions. Thermal models have predicted that the maximum yield of hypernuclei should occur in the collision energy range covered by the STAR FXT program. The thermal model with the canonical ensemble for strangeness [3] can describe the yields of $^{3}_{\Lambda}H$ at both 3 GeV and the ALICE energy 2.76 TeV. But thermal model fails to describe the trend at RHIC energies. UrQMD + coalescence model calculation is consistent with data in these points but still significantly overestimates the data at higher energies.

Particle femtoscopy

A standard method for studying the space and time characteristics of the emitting source created in heavy ion collisions is the two-particle interferometry, also referred to as the femtoscopy [4]. Three dimension correlation femtoscopy in the Longitudinally Co-Moving System (LCMS) is a standard tool to extract the shape of the particle emission region. The relative pair momentum can be projected onto the Bertsch-Pratt [5,6], out-side-long system: out (along the transverse momentum of the pair), long (along the beam direction) and side (perpendicular to longitudinal and outward directions). Femtoscopic radii $R_{out}, R_{side}, R_{long}$ have been extracted from the fit to the correlation function using Bowler–Sinyukov fitting procedure [7,8].

Figure 4 shows dependences of correlation strength (λ) and radii R_{out}, R_{side}, R_{long}, R_{out}/R_{side} ratio and $R^2_{out} - R^2_{side}$ from collision energies for positive and negative pions. The full red and blue stars are the new result of femtoscopic parameters values at four collision energies 3.0, 3.2, 3.5 and 3.9 GeV. Extracted femtoscopic parameters and R_{out}/R_{side}, $R^2_{out} - R^2_{side}$ ratios favor more the trend of HADES and STAR's collider mode results, rather than E895 results.

The first $d - \Lambda$ correlation function measurements in heavy-ion collisions

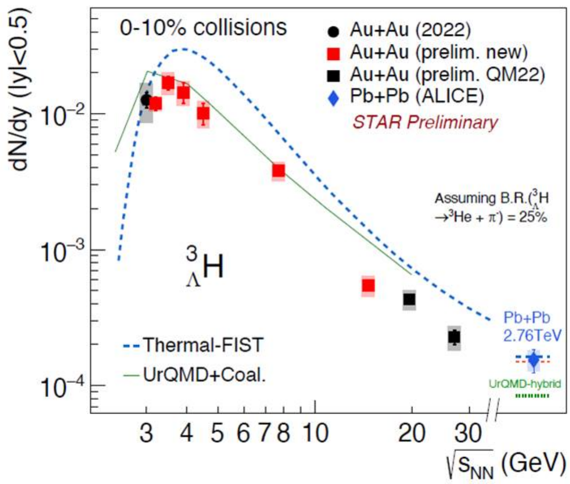

Fig. 3. Dependence of ${}^{3}_{\Lambda}H$ yields within $|\eta| < 0.5$ on the beam energy in $0 - 10\%$ central heavy-ion collisions. The symbols represent STAR and ALICE measurements while the lines represent different theoretical calculations.

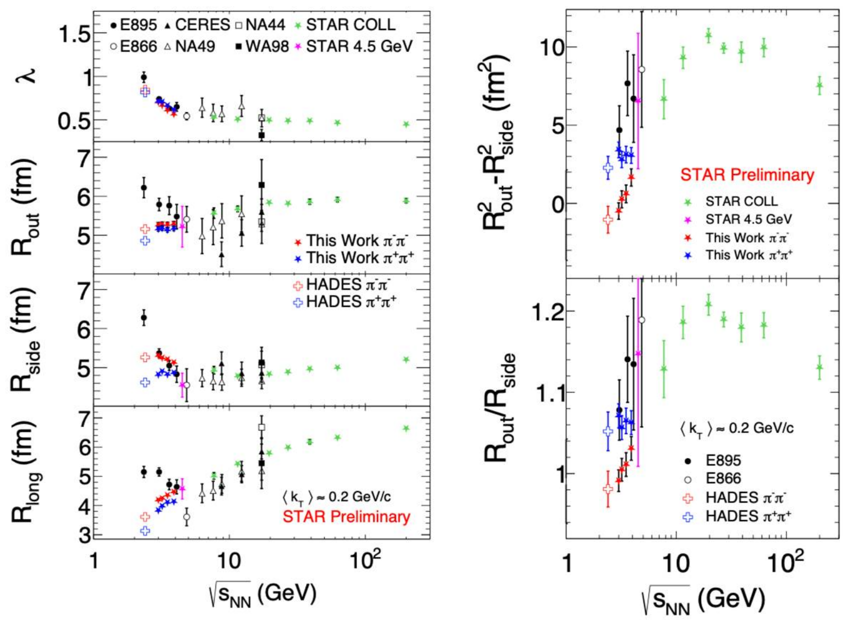

Fig. 4. Dependences of correlation strength (λ) and radii $R_{out}, R_{side}, R_{long}$, R_{out}/R_{side} ratio and $R^2_{out} - R^2_{side}$ from collision energies for positive and negative pions.

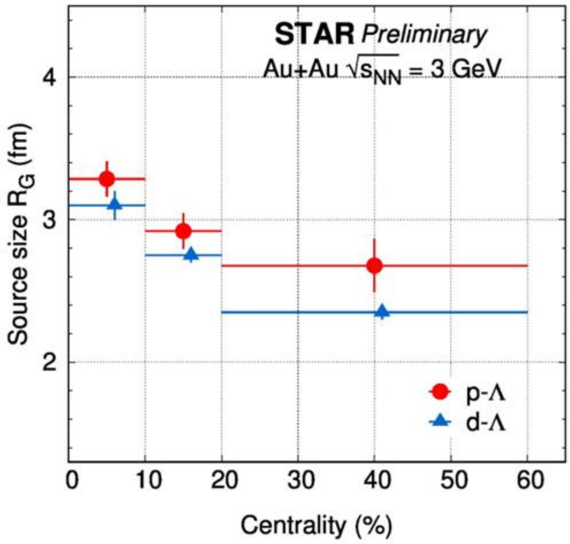

Fig. 5. Dependence source size from the various centralities in $p-\Lambda$ and $d-\Lambda$ correlation function in Au+Au collisions at 3 GeV.

were reported. The Lednicky-Lyuboshitz (L-L) formalism [9] was used to successfully separate emission source size, the scattering length (f_0) and the effective range (d_0) from final state interactions in $p-\Lambda$ and $d-\Lambda$ correlation functions. Figure 5 shows dependence of source size on centrality in $p-\Lambda$ and $d-\Lambda$ correlation functions. Collision dynamics behaves as expected: source size increase from peripheral to central collisions and source size for $p-\Lambda$ is more than for $d-\Lambda$.

Different spin states with different scattering length and effective range parameters for the $p-\Lambda$ and $d-\Lambda$ correlation function were reported. For the $p-\Lambda$ correlation used spin-averaged fit (Singlet+Triplet state) because of current statistics is not enough to separate two spin states. The extracted parameters from $p-\Lambda$ correlation are equal: $f_0 = 2.32^{+0.12}_{-0.11} fm$, $d_0 = 3.5^{+2.7}_{-1.3} fm$. For the $d-\Lambda$ correlation used spin-separated fit (Doublet and Quartet states). Were predicted very different scattering length for doublet and quartet states: $f_0(D) = -20^{+3}_{-3} fm$, $d_0(D) = 3^{+2}_{-1} fm$ and $f_0(Q) = 16^{+2}_{-1} fm$, $d_0(Q) = 2^{+1}_{-1} fm$.

A new way to constrain the ${}^{3}_{\Lambda}H$ structure was reported. Binding energy was extracted using the Effective Range Expansion (ERE) formula with the values of the scattering length and effective range extracted from the $d-\Lambda$ correlation functions. Figure 6 show the binding energy of the ${}^{3}_{\Lambda}H$ is comparison with others experiment results. Newly measured STAR value of the binding energy is in good agreement with the existing measurements.

Global hyperon polarization measurements

Global hyperon polarization in Au+Au collisions over a large range of collision energies was recently measured and successfully reproduced by hydrodynamic and transport models with intense fluid vorticity of the QGP (see Fig. 7). While a naive extrapolation of data trends suggests a increasing polarization as the collision energy is reduced, the behavior of hyperon polar-

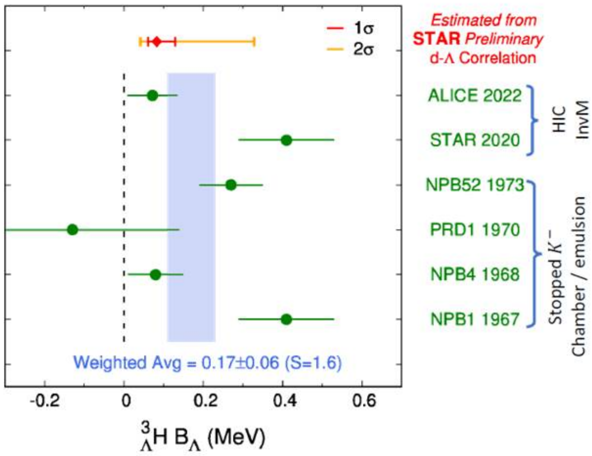

Fig. 6. Comparison the binding energy of the ${}^{3}_{\Lambda}H$ with others experiment results.

ization at very low energy is unknown [11]. STAR has recently measured the polarization of Λ hyperons along the direction of global angular momentum in Au+Au collisions at $\sqrt{s_{NN}} = 3$ GeV. Significant polarization is seen at 3.0 GeV [10]. At 19.6 and 27 GeV, the Lambda and anti-Lambda polarizations are very similar, placing an upper limit on the late-stage magnetic field [12]. The trend of increasing $P_{\rm H}$ with decreasing collision energy is maintained at the low energy for $\sqrt{s_{NN}} = 3$ GeV.

Nuclear modification factor

The nuclear modification factor $\mathrm{R_{cp}}$ will be unity if nucleus-nucleus collisions are just simple superpositions of nucleon-nucleon collisions. Deviation of these ratios from unity would imply contributions from nuclear or in-medium effects. Measurement of the nuclear modification factor $\mathrm{R_{cp}}$ for charged hadrons as well as identified $\pi^{+}(\pi^{-})$, $K^{+}(K^{-})$ and $p(\bar{p})$ for Au+Au collision energies of $\sqrt{s_{NN}} = 7.7$, 11.5, 14.5, 19.6, 27, 39, and 62.4 GeV were carried out using BES-I data [13]. High statistics of BES-II will allow measuring R_{cp} in high transverse momentum region at low collision energies. Figure 8 demonstrates $\mathrm{R_{cp}}$ for Au+Au collision energies 27 GeV in high $\mathrm{p_T}$ region.

Summary

Recent results from the STAR experiment at RHIC were reported. STAR experimental program covers a wide range of topics and STAR has collected a unique set of data on a variety of collision systems and collision energies including fixed target data. STAR completed BES-II data taking, providing 17 unique energies from $\sqrt{s_{NN}} = 3-54.4$ GeV cover the region in $\mu_B \approx 90-720$ MeV with some overlapping collider and FXT energies. STAR BES-II has increased statistics by a factor of 10 for most of the energies and provided additional data with FXT mode of STAR detector. Measurement of ${}^{3}_{\Lambda}H$ and

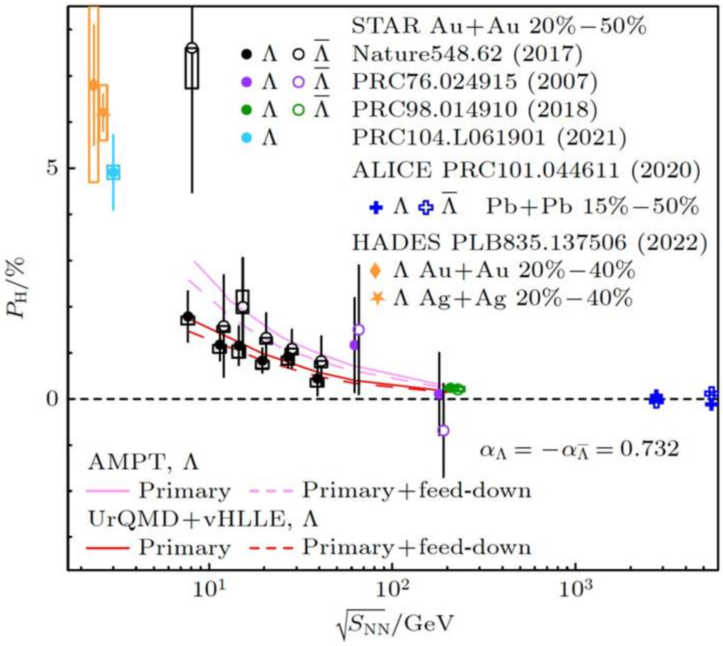

Fig. 7. Global Hyperon (Λ) polarization as a function of $\sqrt{s_{NN}}$ in mid-central heavy-ion collisions.

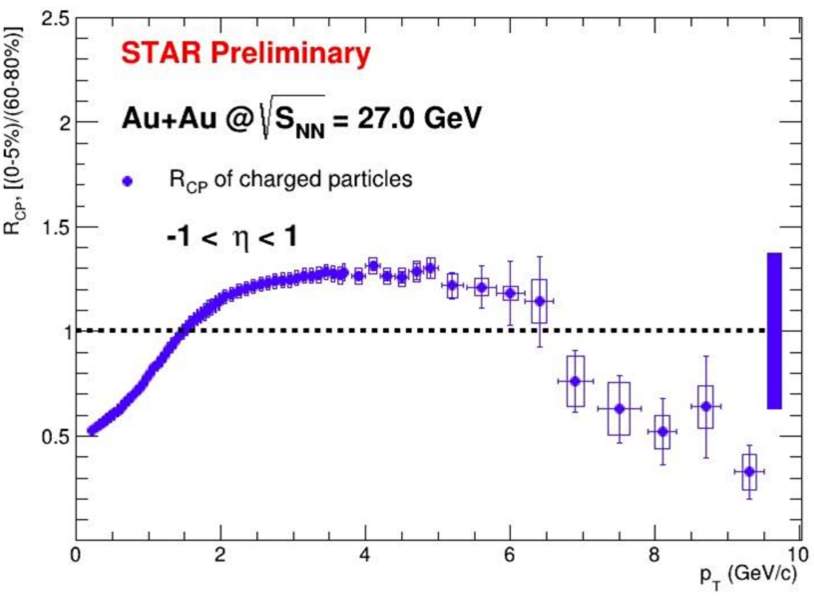

Fig. 8. The nuclear modification factor R_{cp} for Au+Au collision energies 27 GeV.

${}^{4}_{\Lambda}H$ lifetimes have been obtained using the data samples of Au+Au collisions at energies $\sqrt{s_{NN}} = 3$ and 7.2 GeV. The p_T-integrated yields of ${}^{3}_{\Lambda}H$ at mid-rapidity were calculated for central collisions as a function of center-of-mass energy. The first $d-\Lambda$ correlation function measurements in heavy-ion collisions and a new way to constrain the ${}^{3}_{\Lambda}H$ structure were reported. Global hyperon polarization in Au+Au collisions over a large range of collision energies was recently measured and successfully reproduced by hydrodynamic and transport models with intense fluid vorticity of the QGP. High statistics of BES-II will allow measuring R_{cp} in high transverse momentum region at low collision energies. STAR continues to produce highly impactful results for studying the QCD phase diagram and fundamental features of QCD.

Acknowledgments

Author would like to acknowledge that part of the work described in section "Nuclear modification factor" was supported by Russian Science Foundation under grant N 22-72-10028.

REFERENCES

1. M. S. Abdallah et al., [STAR Collaboration], Phys. Rev. Lett. 128, 202301, (2022).
2. J. Adam et al. [ALICE collaboration], Phys. Lett. B 754, 360, (2016).
3. A. Andronic et al., Phys. Lett. B 697, 203, (2011).
4. M. Lisa, S. Pratt, R. Soltz and U. Wiedemann, Ann. Rev. Nucl. Part. Sci. 55, 357, (2005).
5. Pratt S. Pion Interferometry of Quark-Gluon Plasma // Phys. Rev. D. 1986. V. 33. P. 1314-1327.
6. Bertsch G., Gong M., Tohyama M. Pion Interferometry in Ultrarelativistic Heavy Ion Collisions // Phys. Rev. C. 1988. V. 37. P. 1896-1900.
7. Yu. Sinyukov et al., Phys. Lett. B 432, 248, (1998).
8. M. Bowler, Phys. Lett. B 270, 69, (1991).
9. R. Lednicky and V. L. Lyuboshitz, Sov. J. of Nucl. Phys. 35, 770, (1982).
10. M. S. Abdallah et al., [STAR Collaboration], Phys. Rev. C 104, L061901, (2021).
11. Xu. Sun et al.,Acta Phys.Sin. 72, 7, 072401 (2023).
12. M. S. Abdallah et al., [STAR Collaboration], Phys. Rev. C 108, 014910, (2023).
13. L. Adamczyk et al., [STAR Collaboration], Phys. Rev. Lett. 121, 032301, (2018).